Cool Cities: The Value of Urban Trees*

Lu Han Stephan Heblich Christopher Timmins
Yanos Zylberberg

July 17, 2021

Work in Progress

Abstract

This paper estimates the amenity value of urban trees. The empirical strategy exploits an ecological catastrophe—the emerald ash borer (EAB) infestation in Toronto—to isolate exogenous variation in the evolution of the tree canopy across neighborhoods. One additional tree within a postcode increases property prices by 0.5-0.8%; neighborhoods most affected by the EAB infestation experienced a decrease in tree cover of 6 percentage points and a drop in property prices of up to 5%. One dimension of the tree premium relates to the cooling properties of urban trees. We quantify this effect of shade and evapotranspiration on local temperature during heatwaves and on energy consumption. Our findings suggest large, mitigating effects of urban forestry on urban heat and substantial energy savings, which however only explain a small share of the overall amenity value of trees.

Keywords: Environmental amenities; urban heat island; urban green infrastructure.

*Han: University of Toronto and University of Wisconsin, Lu.Han@rotman.utoronto.ca; Heblich: University of Toronto, CESifo, IfW Kiel, IZA, SERC; stephan.heblich@utoronto.ca; Timmins: Duke University, NBER; christopher.timmins@duke.edu; Zylberberg: University of Bristol, CESifo, Alan Turing Institute; yanos.zylberberg@bristol.ac.uk. We would like to thank Piet Eichholtz, Pierre-Philippe Combes, Naomi Hausman, Matthew Kahn, Giacomo Ponzetto, Yu Qin, Stijn Van Nieuwerburgh, John Yinger and Siqi Zheng for helpful comments. The usual disclaimer applies.

Since 2002, the emerald ash borer (EAB) infestation has affected millions of ash trees in North America, with a non-negligible impact on the population of "urban" trees. This ecological catastrophe made salient the social value of green capital in large cities.[1] There are obvious aesthetic benefits of trees in cities, with large externalities within neighborhoods (Benson et al., 1998; Todorova et al., 2004); trees have wind-sheltering properties during the winter (Frank et al., 1981; Akbari and Taha, 1992; Nikoofard et al., 2011; Upreti et al., 2017); they contribute to (road traffic) noise attenuation (Kragh, 1981); and a house surrounded by trees is not overlooked. In addition, there are large temperature differentials between urban areas and the adjacent countryside—a phenomenon known as the *urban heat island* effect (Oke, 1973)—, and the tree canopy alleviates this effect through evapotranspiration and shading. The impact on welfare and energy consumption during high temperature episodes is important to understand, especially so with global warming intensifying urban heat island effects.

This paper estimates the value of urban trees. We rely on comprehensive urban forest and land cover assessments collected in 2001 and 2018 by the City of Toronto in order to evaluate changes in the tree canopy.[2] This ten-year period coincides with the EAB infestation, which we exploit to isolate exogenous variation in the evolution of the tree canopy. Exposure to the EAB infestation can be measured at a local level using a geo-referenced register of all city-managed urban trees, which reports tree species, logged maintenance dates, and tree cut downs.

We first estimate the hedonic value of the tree canopy. We instrument the evolution in the tree canopy within a postcode by its initial exposure to the EAB infestation, and we identify its effect on residential property values using exhaustive data on property transactions between 2007 and 2017. We find that one additional tree within a postcode increases property prices by 0.5-0.8%. As ash trees were unequally planted across neighborhoods, the EAB infestation had widely different effects across the City of Toronto. In some neighborhoods where most city-managed urban trees were ash trees before the infestation, the impact on property values is substantial. For instance, neighborhoods which were most affected by the EAB infestation experienced a 6 percentage points decrease in tree cover and a 5% drop in

[1]The previous infestation of such amplitude was the Dutch elm disease, spreading from 1940 to 1970 in North America. This catastrophe pre-dated the EAB infestation, but it also shaped its impact on cities. Indeed, many cities decided to replace the infested elm trees—the first-best urban tree—with ash trees.

[2]The 2007 data was part of the Urban Tree Canopy (UTC) Assessment conducted by Urban Forestry; the update was titled the 2018 Tree Canopy Study. We complement the data with vegetation and built-up indices constructed between 2007 and 2020 from satellite imagery (Sentinel 2, 2016–2020, Landsat L8, 2013–2020, Landsat L7, 2007–2012).

property prices.

Second, we quantify the role of energy savings in explaining the "tree premium." Heat waves lead to peaks in energy consumption, and these peaks are partly mitigated in neighborhoods with a larger tree canopy. We find that a 10 percentage point additional tree cover within a postcode reduces the average temperature during Summer months (in 2018) by about 2.7% or 0.8 degrees (Celsius) and lowers the average daily energy consumption by about 1.5-2 kilowatt-hours (kWh) which correspond to a monthly saving of CAD 7.5-10.5. We use these estimates to monetize the value of trees in alleviating urban heat island effects under different scenarios, i.e., more and less conservative climate change projections. Our findings suggest substantial energy savings from urban trees, magnified by the expected increase in urban temperature due to climate change. These effects however still represent a small share of the hedonic value of trees, even when these energy savings already exceed the yearly maintenance costs per tree of CAD 4.20 by far (2011 City of Toronto parks and forestry budget proposal).[3]

This paper is not the first one to estimate the hedonic price of urban trees (see Morales, 1980; Conway et al., 2010; Franco and Macdonald, 2018; Wachter and Wong, 2008) and the effect of trees on energy savings (see Akbari and Taha, 1992; Nikoofard et al., 2011). However, the two exercises present one major empirical challenge: omitted variation. For instance, leafy suburbs may benefit from various unobserved amenities (e.g., school quality, peer effects); the opportunity cost of land may be too large in highly-demand and densely-populated neighborhoods to maintain a tree canopy. There would be an upward bias in the correlation between the tree density and property values in the former case versus a downward bias in the latter case. In the same vein, households who live in green neighborhoods might be more concerned about the environment and use less energy than the average household. Our contribution is to overcome this problem and present causal estimates of the hedonic price of urban trees or their effect on energy savings.

The empirical strategy exploits two sources of exogenous variation. Our baseline specification instruments the secular evolution of the tree canopy using an ecologi-

[3]The cooling effect of trees reduces electricity consumption in the summer and their wind sheltering effect reduces natural gas consumption in the winter. To distinguish the specific energy effects of trees surrounding the house from a more general neighborhood effect, we exploit short-term weather fluctuations, in particular heat waves and episodes of wind chill. These fluctuations are interacted with measures of shading and wind-sheltering computed from the positioning of trees relative to each property—these calculations account for solar angles and weekly wind directions over the course of a year. Using panel data on residential electricity meter readings at the postcode/month level from 2011–2015 and natural gas data at the postcode/month level from 2010–2017, we show that the tree canopy substantially affects the elasticity of energy consumption to extreme heat.

cal catastrophe which scarred North-American cities, the EAB infestation.[4] Early infestations in the City of Toronto were detected in 2007, and the city expected to lose nearly all of its 860,000 ash trees within ten years. The loss of these prime shade trees amounts to about 8% of the tree canopy cover over both public and private land. We rely on this ecological catastrophe to isolate large, exogenous changes in the tree canopy between 2007 and 2018. The identification assumption is that the initial allocation of ash trees is orthogonal to the evolution of residential prices, and the dynamics in urban heat and energy consumption at the postcode level—conditioning on the density of city-managed trees.[5]

In an alternative specification, we exploit fluctuations in extreme weather episodes coupled with measures of exposure computed from the positioning of trees around each property. We calculate the *solar-shading potential* of each tree in each month of the year, by combining the relative positioning of the tree and the property with solar angles across the year. We further calculate the *wind-sheltering potential* of each tree in each month of a year by combining the relative positioning of the tree and the property with monthly wind roses. The annual average of these measures may be correlated with general levels of energy consumption, as positions of trees might partly reflect optimization behavior from households. The identifying assumption is that excess energy savings during extreme weather episodes are not directly correlated with either the *solar-shading potential* or the *wind-sheltering potential*—other than through the mitigation effect of trees themselves.

Our research relates to different strands of the literature. First, it contributes to research at the intersection of urban and environmental economics which assesses the value of green urban infrastructure. The (monetary) value of trees has been widely recognized by urban planners and Mullaney et al. (2015) provide a comprehensive review of this literature. Wachter and Wong (2008) is one of the few papers in economics attempting to estimate the value of individual trees using house price hedonics; Franco and Macdonald (2018) extend this to an analysis of the house price effect of tree canopy coverage in Lisbon.[6] We contribute to this literature by

[4]The emerald ash borer is a beetle native to Asia that was accidentally introduced to North America and first discovered near Detroit, MI (USA) and Windsor, ON (Canada) in the summer of 2002. Since then, the emerald ash borer has become one of the most destructive non-native insects in North-America. By 2018, it had spread over 33 states in the U.S. and the Canadian provinces of Ontario, Quebec, and Manitoba and killed hundreds of millions of ash trees (Aukema et al., 2011; Herms and McCullough, 2014). See http://www.emeraldashborer.info/ for ongoing updates on the spread of the EAB pest.

[5]For a similar density of city-managed trees, there exists large variation in the number of ash trees and thus in the number of trees that were lost to the recent EAB infestation. The initial allocation of ash trees in Toronto was partly related to a previous catastrophe, the Dutch elm disease, which had a similar uneven impact on the tree canopy during the 1970s.

[6]Jones and McDermott (2018a) point out that most papers focus on the benefits of trees without

providing plausibly causal estimates of the amenity value of trees.

Second, our analysis focuses on one specific effect of green infrastructure, i.e., its potential to reduce energy consumption during extreme heat events.[7] This part relates to Auffhammer (2018) who assesses how future climate change will affect electricity and natural gas consumption in California. We further relate to work on the economic value of green buildings (Eichholtz et al., 2010, 2013) and energy efficient houses as reviewed in the handbook chapter by Kahn and Walsh (2015).

Lastly, we add to the literature on the effects of climate change on densely populated urban areas (see, for instance, the review articles by Dell et al., 2014; Graff Zivin and Neidell, 2013; Kahn and Walsh, 2015). With urbanization comes an increase in impermeable surfaces like stone, concrete and asphalt, which tend to have high albedo rates. The loss of soil and vegetation reduces the natural cooling effect of evapotranspiration and shading from trees and other vegetation, thus leading to observable temperature differentials between urban areas and the adjacent countryside. Oke (1973) refers to this phenomenon as the *urban heat island* effect. An immediate consequence of heat islands is an increasing energy demand for cooling and, in the presence of climate change, these costs are expected to rise markedly (Estrada et al., 2017; Santamouris et al., 2015). One way to mitigate the urban heat island effect is to invest in the urban canopy.[8] Building energy simulations suggest significant shading effects depending on the orientation, size and distance to urban trees, but effects may differ by season. The same shading may have negative effects during the winter period from reduced solar thermal gains but this can weigh against positive wind-sheltering effects (Frank et al., 1981; Akbari and Taha, 1992; Nikoofard et al., 2011; Upreti et al., 2017).

The remainder of the paper is structured as follows. In Section 1, we describe the context, the data sources and the effect of the EAB infestation on urban forestry. Section 2 presents the empirical strategy. Sections 3 and 4 provide causal estimates of the hedonic price of urban forestry and its effect on urban heat and energy savings. The final section concludes.

consideration of costs. To address this, they develop a bio-economic health model that accounts for a range of benefits, costs and externalities and calibrate it to data from New York City. They report positive yet smaller net benefits of trees than commonly reported in the literature.

[7] Jones and McDermott (2018b) use time-variation in the spread of EAB across U.S counties to estimate how the loss of trees affected level of air pollutants.

[8] Roy et al. (2012) review existing studies on urban tree benefits across different climatic zones and Bowler et al. (2010) provide a more general review of the benefits of urban green infrastructure in general.

1 Context, data and evolution of the tree canopy

This section discusses the original allocation of ash trees across neighborhoods of Toronto and the evolution of the emerald ash borer (EAB) infestation over the past decade. We then describe our data sources and data construction. We finally shed light on the relationship between the EAB infestation and the evolution of the tree canopy, which constitutes the first stage of our baseline empirical strategy.

1.1 Context

Toronto is one of the greenest cities in North America. The 2018 Tree Canopy Study found that Toronto has an estimated 11.5 million trees, as much as the combined number of trees in New York (5.2 million) and Los Angeles (6 million).[9] The tree population in Toronto consists of a large number of native trees, that date back to the Carolinian forests before the 18th century. These species include: black, green and white ash; birch; white cedar; American chestnut; white elm; maple; black, red, white oak; white pine etc. Additional non-native species were introduced by European settlers, e.g., barberry, larch, lilac, Norway maple or pine.

Dutch elm disease and the allocation of trees before 2007 Growing trees in cities is notoriously difficult. Road salt, compact soil, pollution and Canada's winters all make urban areas of Toronto unkind to trees. The tree of choice in such harsh environments used to be elm trees, which thrive in urban areas and present convenient aesthetic features. Elm trees were primarily planted at the beginning of the 20th century in North America, such that their allocation across the city of Toronto coincides with neighborhood growth between 1900 and 1930.

Elm trees steadily disappeared from most North-American cities due to the Dutch elm disease. Around 1930, elm bark beetles appeared in New York, threatening the large population of trees in New Haven. However, the disease did not start to propagate until the Second World War when the quarantine and sanitation procedures that had been implemented since 1928 were abandoned due to budget restrictions. After the Dutch elm disease swept through toward the second half of the last century, most municipalities planted ash trees as a "second-best" urban tree (MacFarlane and Meyer, 2005). The past allocation of elm trees across and within cities of the East

[9] Apart from the central business district and industrial parks, most neighborhoods have alleys of trees or public parks. Houses in rich residential neighborhoods have backyard gardens with significant tree coverage. The city of Toronto estimates a structural value of its urban forest that amounts to CAD 7.04 billion plus ecosystem services worth more than CAD 55 million each year (City of Toronto, 2019).

Coast thus closely relates to the more recent allocation of ash trees. Neighborhoods of Toronto with large populations of elm trees in 1930, e.g., Scarborough or Mount Pleasant, have a large population of ash trees nowadays.

Emerald ash borer infestation The emerald ash borer is a beetle that was accidentally introduced to North America around 2000. This invasive species survives well in the North-American environment, due to a lack of natural predators. The beetle attacks trees at all stages of its life-cycle: the larva feeds aggressively on tissues of the trees, which produces larval galleries and frass; the adults then escape the tree which leaves holes in the bark—one of the first recognizable symptoms of infestation. Adults feed on ash foliage, but only live sufficiently long (less than a month) to lay a cluster of eggs in crevices of the bark. Overall, infested trees present yellow foliage, bark fissures, high woodpecker activity (feeding on borers), larval galleries which can be spotted using holes in the bark (and frass). Without specific treatment, e.g., TreeAzin injections in the very early stages of the infestation, it takes between 1 and 4 years for the infested ash tree to die. Between 2007 and 2017, the city had lost more than half of these 860,000 ash trees.[10]

1.2 Data sources

This section presents the data sources used in this research.

Tree canopy and land cover To estimate the tree cover and its evolution, we use high-resolution land classifications in 2007 and in 2018. These land classifications were performed by the Urban Forestry services of the City of Toronto using multispectral QuickBird satellite imagery at a resolution of 0.6m. The analysis was additionally assisted by LiDAR information, manual assessments and corrections (City of Toronto, 2019). The land classifications isolate the following eight categories: tree canopy, grass/shrub, bare earth, water, buildings, roads, other paved surfaces and agriculture. Figure 1 provides an illustration of such land categories across two neighborhoods of Scarborough in 2007. We combine the land classifications in 2007 and 2018 with the shapes of postcodes to construct the area shares of all categories within the different postcodes (using a buffer of 10m in the baseline specification to properly capture street trees in front of houses).[11]

[10]Removals were concentrated in Scarborough, North York and Etobicoke. Trees in Downtown Toronto received early TreeAzin injections, possibly delaying or preventing their full infestation.

[11]To facilitate the calculations of the solar-shading or wind-sheltering potential, we transform the "tree cover" surface into a discrete number of individual trees. More specifically, we construct synthetic trunk locations by randomizing tree trunks every 10 meters inside the "tree coverage"

While the city aimed at harmonizing the classification techniques in 2007 and 2018, there may still be measurement error in the assessed evolution of the tree canopy. Our main empirical strategy should correct for the possible attenuation bias associated with classification errors to some extent. We complement and validate these measures of land cover with vegetation and built-up indices constructed between 2007 and 2020 from satellite imagery (Sentinel 2, 2016–2020, Landsat L8, 2013–2020, Landsat L7, 2007–2012). We describe the construction of these indices and a few validation exercises in Appendix A.1 and shed some light on the evolution of the tree canopy in Appendix A.2.

Ash trees To identify the location of ash trees, we rely on the register of all publicly maintained street trees provided by the City of Toronto (about 600,000 trees in total, and 30,000 ash trees). The data contains the street address, the common tree species and the diameter at breast height which can be used to infer the tree size and also the crown size. For the latter, we rely on estimates of the relationship between the crown diameter and stem diameter (Peper et al., 2014) and use the diameter at breast height to approximate the area that the crown covers.

A specific register focuses on ash trees and the activity related to the EAB infestation, i.e., the dates of EAB Removals and TreeAzin Injections. Figure 1 shows the location of publicly maintained ash trees across two neighborhoods of Scarborough, one with a relatively low density of ash trees and one with a relatively high density of ash trees. To provide additional insight into the distribution of ash trees in the City of Toronto, we show a density map of these publicly maintained ash trees in panel (a) of Figure 2. While ash trees are present in every ward, they are most concentrated in the North-East of the city.

Property values We use exhaustive property transaction data between 2007 and 2017 in order to estimate the hedonic value of the local tree canopy. The data comes with a wide range of transaction and property attributes: the transaction date; price; type of property (35 categories); number of floors; number of bedrooms, kitchens, washrooms, family rooms, and fireplaces; the size of the lot; and parking space. The dataset contains about 387,000 transactions (between 30,000-40,000 per year). To geolocate properties, we combine the transaction data with a geolocated address register provided by the City of Toronto, and perform a fuzzy string matching algorithm on addresses. Panel (b) of Figure 2 shows the overall distribution of transactions within the City of Toronto between 2007 and 2017. In order to correct

surface.

for the over-representation of transactions in certain neighborhoods, e.g., downtown Toronto, the main empirical strategy will weigh each transaction to equalize the overall weight of each postcode.

We complement the transaction data with neighborhood characteristics from the cadastre of the City of Toronto that includes detailed information about property boundaries, building footprints, and the general urban infrastructure. We employ this cartographic information to calculate distance to amenities and other controls capturing neighborhood quality.

Energy consumption and temperature We have access to data from all residential electricity meters in the City of Toronto. About 800,000 customer IDs i are nested in 21,000 postcodes p over the period 2011–2015. We also collect data on the aggregate consumption of natural gas per postcode and month over the period 2010 to 2017; we divide the total gas consumption in a year by the number of registered gas meters to derive a measure of average household gas consumption.[12]

Finally, we collect the Land Surface Temperature (LST) during Summer 2018 using the Thermal Infrared (TIRS) band provided by Landsat L8 and collapse the measure at the level of postcodes, T_p. Specifically, we calculate the Top of Atmospheric (TOA) spectral radiance, convert this brightness measure into a temperature measure and correct for land surface emissivity (LSE). Note that the LSE employs a fractional vegetation measure that is based on the Normalized Difference Vegetation Index (NDVI) (see Ermida et al., n.d., for more details). This might induce some mechanical correlation with the presence of trees, but the LST is currently the best measure to capture surface temperature at a fine spatial scale.

1.3 EAB infestation and the tree canopy

We now discuss important evidence on the effect of the EAB infestation on land cover, mirroring the initial distribution of ash trees across neighborhoods (see Figures 1 and 2).

We first provide an illustration of the systematic removal of infested ash trees by focusing on the North-East of Toronto (the municipal area of Scarborough) where we observe a relatively high density of publicly maintained ash trees at baseline. Figure 3 compares the land classifications provided by Urban Forestry in 2007 (panel a) and in 2018 (panel b). As apparent from the figure, there is a marked decrease in

[12]There are important seasonal patterns in energy consumption. We describe these patterns in Appendix A.3, in which we also discuss the construction of harmonized energy consumption measures at the postcode level.

the area covered by trees which coincides with the location of street ash trees (green symbols).

The systematic relationship between ash trees and tree removals between 2007 and 2018 is further explored in Figure 4. We consider a postcode as the main unit of observation, and we construct the long difference in area share of tree cover between 2007 and 2018. Panel a of Figure 4 shows the correlation between the evolution of the tree canopy (difference in area shares of tree cover within a 10m buffer) and a measure of ash tree density (number of street ash trees per area within a 10m buffer, as measured in 2010) across postcodes. Panel b of Figure 4 conditions this relationship on a measure of street tree density (irrespective of their species), latitude, longitude, the land classification in 2007 (the area shares of tree canopy, grass/shrub, bare earth, water, buildings, roads, other paved surfaces and agriculture) and ward fixed effects. We find that there is a strong, precisely estimated, negative correlation between tree cover in 2018 and the density of ash trees: an additional 0.002 ash trees per square meter is associated with a decrease of 0.06 in the area share of tree cover (see panel b). To rationalize the previous relationship, an additional 0.002 ash tree per square meter corresponds to 2,000 ash trees per square kilometer. If each ash tree uniquely covered about 50-80 square meters (for a crown with a 4-5 meter radius), these 2000 ash trees would cover 10-16% of a square kilometer. Compared to this back-of-the-envelope calculation, the actual tree cover decreases by only 6% of a square kilometer. The difference between the two numbers could be explained by: (i) overlap between tree crowns, (ii) sluggish tree removals and trees having received TreeAzin injections, or (iii) fast replacement.

Our empirical strategy hinges on the intuition that the negative relationship between street tree density and tree removals between 2007 and 2018 is mostly visible with ash trees but not with other species of trees. We explore the relationship between the evolution of the tree canopy between 2007–2018 and the density of publicly maintained trees in Table 1. In this table, as in Figure 4, the unit of observation is a postcode, the dependent variable is the change in tree cover between 2007 and 2018, and we control for ward fixed effects, latitude and longitude, and area shares of trees, grass/shrub, bare earth, water, buildings, roads, other paved surfaces and agriculture in 2007. In column 2, we add a control for the density of all publicly maintained trees within a 10m buffer of the postcode. In column 3, we add the densities of other popular species of publicly maintained trees (i.e., spruce trees, elm trees, maples). The negative effect of the initial density of ash trees is robust across specifications and is one order of magnitude larger than the effects of other tree species. This effect is key to our empirical strategy.

2 Empirical Strategy

This section describes the empirical strategy and a few descriptive statistics.

2.1 Estimating the hedonic value of the tree canopy

The hedonic value of urban forestry should encompass all the net present benefits of a tree in a given proximity to a property, including its long-term effect on energy consumption. An empirical strategy aiming to estimate the causal effect of trees on property values should exploit exogenous and permanent shocks to the tree canopy. The shock used in this paper is the density of public ash trees that were lost to the emerald ash borer infestation and that strongly affected the change in the tree cover between 2007 and 2018 (as documented in the previous section).

A naive empirical strategy would exploit the observed change in the tree canopy over time. Letting i denote a property, t denote a certain year, and p a postcode, we could estimate:

$$\ln(P_{ipt}) = \alpha + \beta TD_{pt} + \gamma \mathbf{X}_{it} + \eta_p + \mu_t + \varepsilon_{ipt}$$

where P_{ipt} is the transaction price, TD_{pt} is the tree cover calculated from its area share within a radius of 10 meters from the shape of a postcode, $\mathbf{X}_{ipt}$ are property characteristics and other time-varying controls (e.g., differential dynamics across: wards, latitude, longitude, the initial land cover in 2007), μ_t are year fixed-effects and η_p are postcode fixed-effects.

This specification suffers from three major issues: omitted variation, reverse causality, and measurement error. First, the evolution of the tree canopy over time may relate to local developments, for instance, investments in green infrastructure, transport infrastructure, or the construction of new offices. These local developments would strongly affect property prices and lead to a local expansion or—more likely—to a reduction of the tree canopy. Second, a rise in the local price of land increases the opportunity cost of maintaining urban forestry. Third, time-variation in our measure of tree density, TD_{pt}, may reflect measurement error induced by differences in the procedures employed to evaluate the tree canopy in 2007 and in 2017. The latter issue is likely to bias the estimated β downward.

We address these identification issues by isolating variation in the tree canopy generated by a permanent and exogenous shock: the emerald ash borer infestation. Letting A_{pt} denote the density of publicly managed ash trees within 10m of a certain

postcode p at time t, we estimate:

$$\ln(P_{ipt}) = \alpha + \beta TD_{pt} + \gamma_{\mathbf{t}}\mathbf{X}_{ipt} + \eta_p + \varepsilon_{ipt} \tag{1}$$

where TD_{pt} is instrumented by A_{pt}, and $\mathbf{X}_{ipt}$ captures the evolution of the time-varying premium associated to observable house characteristics (i.e., number of bedrooms and number of washrooms) and interactions between year fixed effects and ward fixed effects; a measure of street tree density; latitude and longitude; and area shares from the land classification in 2007 (tree canopy, grass/shrub, bare earth, water, buildings, roads, other paved surfaces and agriculture). The specification thus flexibly controls for the differential evolution of prices across neighborhoods and time-varying returns to house characteristics. Standard errors are by default clustered at the postcode × year level. In robustness checks, we consider alternative clustering strategies.

Equation (1) requires measures that capture the evolution of tree density, TD_{pt}, and ash tree density, A_{pt}. We do not have detailed information on the yearly evolution of the tree canopy: we only observe it at the time of the surveys conducted in 2007 and 2018. We do however observe less precise measures of land cover at the yearly level sourced from satellite imagery (see Appendix A.2 where we use these measures to better understand when the urban forestry is visibly affected by tree removals) and we know from records of the City of Toronto that the year 2011 is the beginning of work orders to remove ash trees that were infested with the emerald ash borer.[13] We thus construct the baseline exposure to urban forestry and the baseline instrument as follows: $TD_{pt} = TD_{p,2007}$ for $t \leq 2011$ and $TD_{pt} = TD_{p,2018}$ for $t \geq 2014$, $A_{pt} = A_{p,2010}$ for $t \leq 2011$ and $A_{pt} = 0$ for $t \geq 2014$, and we interpolate linearly for both measures between 2011 and 2014.

One assumption behind our strategy is that all publicly managed ash trees were indeed lost; imperfect "compliance" from the few trees that were "vaccinated" would therefore lead to an under-estimate of the hedonic value of urban forestry. Note that, with forward-looking agents capitalizing the future flow of amenities provided by urban forestry, property prices should reflect future tree removals once the information about the EAB infestation becomes public. We provide robustness checks with alternative cut-offs and without any inference to show that these choices are not driving our main findings. For instance, we can focus on a subsample of property transactions covering (i) a *pre-treatment period* between 2007–2009, where no EAB-related

[13] We observe one work order for an ash tree removal in 2010; 1,646 work orders for ash tree removals in 2011; 3,912 in 2012 and 7,151 in 2013. Unfortunately, we do not have data for later years.

damages had occurred yet; and (ii) a *post-treatment period* between 2016–2017 when the majority of ash trees had been removed.

The identification of specification (1) hinges on the assumption that the initial allocation of ash trees is orthogonal to the evolution of residential prices at the postcode level—conditioning on the evolution of property prices related to the overall number of public trees. This empirical strategy may be threatened by the possible correlation between the spatial distribution of ash trees, inherited from the earlier spatial distribution of elm trees, and neighborhood dynamics in the City of Toronto. For instance, neighborhoods may go through long cycles related to the age of the housing stock (Brueckner and Rosenthal, 2009), and growing neighborhoods in the 1930s may suffer from gentrification and the redevelopment of the historic city center. While we control for dynamics of housing prices at the ward level, we provide a more direct test for this identification threat by assessing the existence of pre-treatment differential trends between 2002 and 2006.

2.2 Descriptive statistics

Before we move on to the estimations, this subsection provides some descriptive statistics that aim to provide a better understanding of the variation underlying the identification strategy.

We start by reporting simple descriptive statistics in Table 2 about transaction data: the mean and standard deviations of the main variables, control variables and their values for transactions with above- and below-median tree canopy. As apparent in Table 2, there are wide differences in tree density across properties. Properties with above-median tree density have almost six times more tree cover than properties with below-median tree density in 2007. Urban forestry correlates with property prices, which are about 40% higher for properties with above-median tree density. This price differential may illustrate a tree premium, but they also seem to indicate differential property characteristics. Properties with above-median tree density have, on average, 0.6 additional bedrooms and one additional washroom.

Figure 5 shows the correlation between house prices and the surrounding urban forestry. The x-axis is our preferred measure of tree cover, TD_{pt}, i.e., the area share of tree cover within 10m of the postcode; and the y-axis is the average (log) house price. The association between transaction prices and tree density should reflect the price premium associated with leafy suburbs, but also the opportunity cost of maintaining urban forestry. As shown in panel (a) of Figure 5, this correlation is positive for almost any share of tree cover in 2007, but especially so in residential areas with some urban forestry. Panel (b) displays the same relationship conditioning

on our main control variables: the number of bedrooms and washrooms; latitude, longitude; and ward fixed effects—all interacted with year fixed effects. As apparent, the price gradient between less and more leafy neighborhoods is linear.

Figure 6 shows the correlation between summer temperatures between June and September (2018), T_p, and the surrounding urban forestry. The figure shows a negative relationship with an average difference of about four degrees Celsius between postcodes with very low versus very high tree cover. This holds true even when conditioning on ward fixed effects and our baseline controls. In the following sections, we will discuss whether this (large) temperature gradient can explain the hedonic value of urban forestry.

3 The hedonic value of urban trees

In this section, we estimate the hedonic value of urban forestry. Our headline finding is that the tree premium is both economically and statistically significant: adding one tree within a postcode increases property prices by 0.5-0.8%.

3.1 Baseline specification

Table 3 reports the estimates of Equation (1). By default, all estimations are conditioned on postcode fixed-effects and year fixed effects interacted with eight categories of land cover in 2007, public tree density, latitude, longitude, and ward-fixed effects. These controls clean for differential price dynamics across neighborhoods. Column 1 reports OLS estimates conditioning on these baseline controls. Column 2 and 3 report IV estimates in which the evolution in tree density between 2007 and 2018, TD_{pt}, is instrumented by the initial density of ash trees, A_{pt}. In column 3, we add transaction controls, including the number of bedrooms and washrooms interacted with year fixed effects to control for valuations of house characteristics that are allowed to vary flexibly over time.

The OLS specification shows that the conditional correlation between tree density and property values is negative and quantitatively irrelevant (column 1). The IV specification finds a positive and significant effect of urban forestry on property prices (columns 2 and 3). One percentage point in land cover within a postcode increases property values by 0.86% in our preferred specification. To help understand the magnitude of these estimates, consider the following thought experiment: one additional (ash) tree within a postcode will increase the land cover by about 50-80 square meters if the crown radius is about 4-5 meters; the average postcode covers about 8,000 square meters; thus, one additional tree increases land cover by 0.6-1

percentage points. This additional tree would cause a property price increase of about 0.5-0.8%. This estimate is unlikely to be affected by a weak-instrument issue, as the first stage is very strong (as shown in Figure 4 and Table 1) and robust to property controls.

3.2 Identification and robustness checks

One threat to identification is that the initial distribution of ash trees, partly reflecting urban developments in the 1930s and the associated distribution of elm trees, correlates with secular neighborhood dynamics. We reduce concerns about this identification threat by testing for the existence of pre-treatment differential trends. Specifically, we consider the period 2002–2006 in which we do observe property transactions, albeit with limited transaction controls, and estimate Equation (1) on this sample of transactions pretending treatment had occurred in between 2004 and 2005. It is reassuring that Table 4 shows no differential trends along the treatment exposure before the treatment date. More specifically, the OLS estimate (column 1) is similar to that obtained on the baseline sample, but the IV estimate (column 2) is small, negative, and non-significant.

We then provide a systematic sensitivity analysis around the baseline specification in Table 5. In Panel A, we construct the baseline exposure to urban forestry and the baseline instrument as follows: $TD_{pt} = TD_{p,2007}$ for $t \leq T_1$ and $TD_{pt} = TD_{p,2018}$ for $t \geq T_2$, $A_{pt} = A_{p,2010}$ for $t \leq T_1$ and $A_{pt} = 0$ for $t \geq T_2$. However, we do not interpolate between T_1 and T_2 and rather exclude the years in between. In short, this specification is equivalent to defining a pre-treatment period $[2007, T_1]$ and a post-treatment period $[T_2, 2017]$. Panel A shows that our main estimate varies between 0.7 and 0.9, when the pre-treatment period changes from $[2007, 2011]$ to $[2007, 2009]$ (and the post-treatment period from $[2014, 2017]$ to $[2016, 2017]$). In Panel B, we consider a long difference setting, similar in essence to the previous exercise, but rather collapse the data at the postcode level. The estimated equation is:

$$\Delta \ln(P_p) = \alpha + \beta TD_{p,2018} + \gamma \mathbf{X}_p + \varepsilon_p \tag{2}$$

where $TD_{p,2018}$ is instrumented by $A_{p,2010}$, and controls (e.g., transaction characteristics, land cover in 2007) are collapsed at the postcode level. As in Panel A, our main estimate varies between 0.7 and 1 when we change the pre-treatment period from $[2007, 2011]$ to $[2007, 2009]$ (and the post-treatment period from $[2014, 2017]$ to $[2016, 2017]$). In Panel C, we consider minor alterations around our baseline specification: we construct land cover and ash tree density with a 20m buffer in column 1

(instead of 10m in the baseline); we winsorize non-zero values for ash tree density and all street tree density at 90% or 99% rather than at 95% in the baseline. Again, the exercise confirms the robustness of our baseline estimations. Lastly, in Panel D, we consider alternative clustering procedures: at the postcode level in column 1; at the ward × year level in column 2; and at the ward level in column 3. Even in the most demanding specification (in column 3) that clusters on the level of about 50 wards, our estimated effects remain precise.

4 The cooling effect of urban forestry

The previous section 3 has shown that there is a significant and positive amenity value to local urban forestry. One possible component of this value derives from the cooling effect of the tree canopy during heat waves. We explore this specific effect in two steps by first looking at local temperatures during heatwaves and then analyzing energy consumption.

Urban forestry and urban heat Urban forestry arguably reduces the urban heat island effects (Oke, 1973; Roy et al., 2012). Our experiment provides a natural setting to quantify such an effect, as we isolate exogenous variation in the evolution of the tree canopy within postcodes over time.

Figure 7 illustrates the correlation between urban temperature and urban forestry. We construct an average mosaic of Landsat 8 satellite imagery for the period 1 June 2018 to 30 September 2018 and consider two indices based on the relative reflectance of different bands: the Normalized Difference Vegetation Index (NDVI) capturing vegetation cover; and the Land Surface Temperature (LST) which we also calculate at a 30-meter spatial resolution.[14] The left panel of Figure 7 displays the average NDVI over the period, and the right panel shows the average LST across two adjacent neighborhoods with significant differences in tree canopy coverage (South Parkdale, South-West of Toronto). We observe a sharp difference between the West and the East of Dufferin St: the tree coverage in the West of Dufferin St markedly alleviates the rise in temperature during this heat wave episode.

To investigate this relationship more formally, we consider the following specification where each observation is a postcode (see Table 6),

$$\ln(T_{p,2018}) = \alpha + \beta TD_{p,2018} + \gamma \mathbf{X}_p + \varepsilon_p \tag{3}$$

[14] As mentioned in section A, the two measures share some mechanical correlation because the LST calculations employ a fractional vegetation measure that is based on the ratio of the maximum and minimum values of the NDVI to correct the temperature measure derived from the Thermal Infrared (TIRS) band.

where $T_{p,2018}$ is the average Land Surface Temperature within postcode p, and urban forestry in 2018, $TD_{p,2018}$, is instrumented by the density of ash trees in 2010, $A_{p,2010}$. Controls include: ward fixed effects (columns 1-3); latitude and longitude (columns 2-3); the density of publicly maintained trees (columns 2-3); area shares from the land classification in 2007 (columns 2-3); and the (log) temperature in 2018 (column 3). As shown in Table 6, urban forestry significantly reduces urban heat during summer months: a 10 percentage point additional tree cover within a postcode reduces temperature by about 2.7% or 0.8 degrees (Celsius). Global warming is expected to increase temperatures across neighborhoods in Toronto; the previous exercise sheds some light on the value of trees in reducing urban heat island effects in the future.

Urban forestry and energy savings Urban forestry reduces the urban temperature during the warm summer months; this should affect energy consumption through the (lower) use of air conditioning.

We investigate this energy saving effect in Table 7 where we consider specification (3) and replicate the exercise performed in Table 6 with the electricity differential between Summer (June, July, August) versus the other months as the main dependent variable. One shortcoming is that we do not observe energy consumption at the beginning and end of the treatment period, but for intermediate years (2011–2015). We thus consider the electricity differential in 2014 (top panel) and in 2015 (bottom panel), controlling for the electricity differential in 2011 (column 3). Table 6 shows that a 10 percentage point additional tree cover within a postcode reduces the average daily energy consumption during the Summer months by about 1.5-2 kilowatt-hours (kWh) which correspond to 25-35 cents and CAD 7.5-10.5 per month. Even though these energy savings are substantial, the discounted cumulative energy savings remain at most in the low thousands which is one order of magnitude too small to explain the amenity value of urban forestry derived in Section 3.

We provide in Appendix B an alternative specification exploiting short-term weather fluctuations interacted with solar exposure induced by the positioning of trees and solar angles. We also characterize the sheltering effect of urban forestry during Winter months.

In summary, we show that trees play a role in reducing heat effects in the summer and they can also provide shelter from wind in the winter. For the individual house, we find that this has a direct monetary value that comes from the reduction in energy and gas expenditures and we expect these savings to become more relevant in the future as temperatures and energy prices may rise. That said, it is not surprising

that these direct monetary benefits do not explain the overall amenity value of trees since previous research has shown that trees provide additional amenity effects that are also capitalized in house prices.

5 Concluding remarks

This paper assesses the value of urban trees. We first estimate the hedonic price of urban trees. This exercise is challenging because the correlation between tree density and property prices could reflect local redevelopments or the opportunity cost of maintaining urban forestry. To establish causality, we rely on large, quasi-experimental variation deriving from the emerald ash borer infestation in Toronto that wiped out a significant share of the tree canopy between 2011 and 2018. We find that the hedonic price of urban forestry is positive and large.

Existing research has shown that trees have a number of beneficial effects on their environment which may contribute to this estimated amenity effect. For instance, Kardan et al. (2015) have highlighted the positive effect of trees on mental health in a study that uses the 2007 canopy survey in Toronto, and a recent study by Jones and McDermott (2018b) analyzes how the loss of ash trees leads to increased air pollution. Less research has systematically analyzed the energy savings from the urban tree canopy. We use novel data on households electricity and gas consumption and find that trees reduce the local temperature during heat waves, leading to a reduction in energy consumption. In the next steps, we plan to quantify how much of the energy effect of trees is driven by temperature reduction and to combine information on temperature predictions for the year 2050 with the city's goal to grow the tree canopy over the next decade in order to assess the role of urban forestry in alleviating urban heat island effects and their impact on energy consumption.

References

Akbari, H. and H. Taha, "The impact of trees and white surfaces on residential heating and cooling energy use in four Canadian cities," *Energy*, 1992, *17* (2), 141–149.

Auffhammer, Maximilian, "Climate Adaptive Response Estimation: Short And Long Run Impacts Of Climate Change On Residential Electricity and Natural Gas Consumption Using Big Data," NBER Working Papers 24397, National Bureau of Economic Research, Inc 2018.

Aukema, Juliann E., Brian Leung, Kent Kovacs, Corey Chivers, Kerry O. Britton, Jeffrey Englin, Susan J. Frankel, Robert G. Haight, Thomas P. Holmes, Andrew M. Liebhold, Deborah G. McCullough, and Betsy Von Holle, "Economic impact of non-native forest pests in the continental United States," *PLoS One*, 2011, *6* (9).

Benson, Earl D, Julia L Hansen, Arthur L Schwartz, and Greg T Smersh, "Pricing residential amenities: the value of a view," *The Journal of Real Estate Finance and Economics*, 1998, *16* (1), 55–73.

Bowler, Diana E., Lisette Buyung-Ali, Teri M. Knight, and Andrew S. Pullin, "Urban greening to cool towns and cities: A systematic review of the empirical evidence," *Landscape and Urban Planning*, 2010, *97* (3), 147–155.

Brueckner, Jan K and Stuart S Rosenthal, "Gentrification and neighborhood housing cycles: will America's future downtowns be rich?," *The Review of Economics and Statistics*, 2009, *91* (4), 725–743.

City of Toronto, "2018 Tree Canopy Study," Technical Report, Report from the General Manager, Parks, Forestry and Recreation 2019.

Conway, Delores, Christina Q Li, Jennifer Wolch, Christopher Kahle, and Michael Jerrett, "A spatial autocorrelation approach for examining the effects of urban greenspace on residential property values," *The Journal of Real Estate Finance and Economics*, 2010, *41* (2), 150–169.

Dell, Melissa, Benjamin F. Jones, and Benjamin A. Olken, "What Do We Learn from the Weather? The New Climate-Economy Literature," *Journal of Economic Literature*, September 2014, *52* (3), 740–98.

Eichholtz, Piet, Nils Kok, and John M. Quigley, "Doing Well by Doing Good? Green Office Buildings," *American Economic Review*, 2010, *100* (5), 2492–2509.

_ , _ , and _ , "The Economics of Green Building," *The Review of Economics and Statistics*, 2013, *95* (1), 50–63.

Ermida, Sofia L., Patrícia Soares, Vasco Mantas, Frank-M. Göttsche, and Isabel F. Trigoe, "Google Earth Engine open-source code for Land Surface Temperature estimation from the Landsat series.," *Remote Sensing*, *12*.

Estrada, Francisco, W. J. Wouter Botzen, and Richard S. J. Tol, "A global economic assessment of city policies to reduce climate change impacts," *Nature Climate Change*, 2017, *7*, 403–406.

Franco, Sofia F and Jacob L Macdonald, "Measurement and valuation of urban greenness: Remote sensing and hedonic applications to Lisbon, Portugal," *Regional Science and Urban Economics*, 2018, *72*, 156–180.

Frank, Randall S., R.Bruce Gerding, Patricia A. O'Rourke, and Werner H. Terjung, "Simulating urban obstructions," *Simulation*, 1981, *36* (3), 83–92.

Herms, Daniel A. and Deborah G. McCullough, "Emerald ash borer invasion of North America: history, biology, ecology, impacts, and management," *Annual Review of Entomology*, 2014, *59*, 13–30.

Jones, Benjamin A. and Shana M. McDermott, "The economics of urban afforestation: Insights from an integrated bioeconomic-health model," *Journal of Environmental Economics and Management*, 2018, *89*, 116–135.

_ **and** _ , "Health Impacts of Invasive Species Through an Altered Natural Environment: Assessing Air Pollution Sinks as a Causal Pathway," *Environmental and Resource Economics volume*, 2018, *71*, 23–43.

Kahn, Matthew E. and Randall Walsh, "Cities and the Environment," in Gilles Duranton, J. V. Henderson, and William C. Strange, eds., *Handbook of Regional and Urban Economics*, Vol. 5 of *Handbook of Regional and Urban Economics*, Elsevier, 2015, pp. 405–465.

Kardan, Omid, Peter Gozdyra, Bratislav Misic, Faisal Moola, Lyle J. Palmer, Tomáš Paus, and Marc G. Berman, "Neighborhood greenspace and health in a large urban center," *Scientific Reports*, 2015, *5* (11610).

Kragh, J, "Road traffic noise attenuation by belts of trees," *Journal of Sound and Vibration*, 1981, *74* (2), 235–241.

MacFarlane, David W and Shawna Patterson Meyer, "Characteristics and distribution of potential ash tree hosts for emerald ash borer," *Forest Ecology and Management*, 2005, *213* (1-3), 15–24.

Mohareb, Eugene A. and Adrian K. Mohareb, "A comparison of greenhouse gas emissions in the residential sector of major Canadian cities," *Canadian Journal of Civil Engineering*, 2014, *41* (4), 285–293.

Morales, Dominic J, "The contribution of trees to residential property value," *Journal of Arboriculture*, 1980, *6* (11), 305–308.

Mullaney, Jennifer, Terry Lucke, and Stephen J. Trueman, "A review of benefits and challenges in growing street trees in paved urban environments," *Landscape and Urban Planning*, 2015, *134*, 157–166.

Nikoofard, Sara, V. Ismet Ugursal, and Ian Beausoleil-Morrison, "Effect of external shading on household energy requirement for heating and cooling in Canada," *Energy and Buildings*, 2011, *43* (7), 1627 – 1635.

Oke, T.R., "City size and the urban heat island," *Atmospheric Environment*, 1973, *7* (8), 769–779.

Peper, Paula J., Claudia P. Alzate, John W. McNeil, and Jalil Hashemi, "Allometric equations for urban ash trees (Fraxinus spp.) in Oakville, Southern Ontario, Canada," *Urban Forestry & Urban Greening*, 2014, *13* (1), 175–183.

Roy, Sudipto, Jason Byrne, and Catherine Pickering, "A systematic quantitative review of urban tree benefits, costs, and assessment methods across cities in different climatic zones," *Urban Forestry & Urban Greening*, 2012, *11*, 351–363.

Santamouris, M., C. Cartalis, A. Synnefa, and D. Kolokotsa, "On the impact of urban heat island and global warming on the power demand and electricity consumption of buildings: A review," *Energy and Buildings*, 2015, *98*, 119–124. Renewable Energy Sources and Healthy Buildings.

Todorova, Assenna, Shoichiro Asakawa, and Tetsuya Aikoh, "Preferences for and attitudes towards street flowers and trees in Sapporo, Japan," *Landscape and urban planning*, 2004, *69* (4), 403–416.

Upreti, Ruby, Zhi-Hua Wang, and Jiachuan Yang, "Radiative shading effect of urban trees on cooling the regional built environment," *Urban Forestry and Urban Greening*, 2017, *26*, 18–24.

Wachter, Susan M. and Grace Wong, "What Is a Tree Worth? Green-City Strategies, Signaling and Housing Prices," *Real Estate Economics*, 2008, *36* (2), 213–239.

Zivin, Joshua Graff and Matthew Neidell, "Environment, Health, and Human Capital," *Journal of Economic Literature*, September 2013, *51* (3), 689–730.

Figures and Tables

Figure 1. Land use classification in 2007 and (public) ash trees.

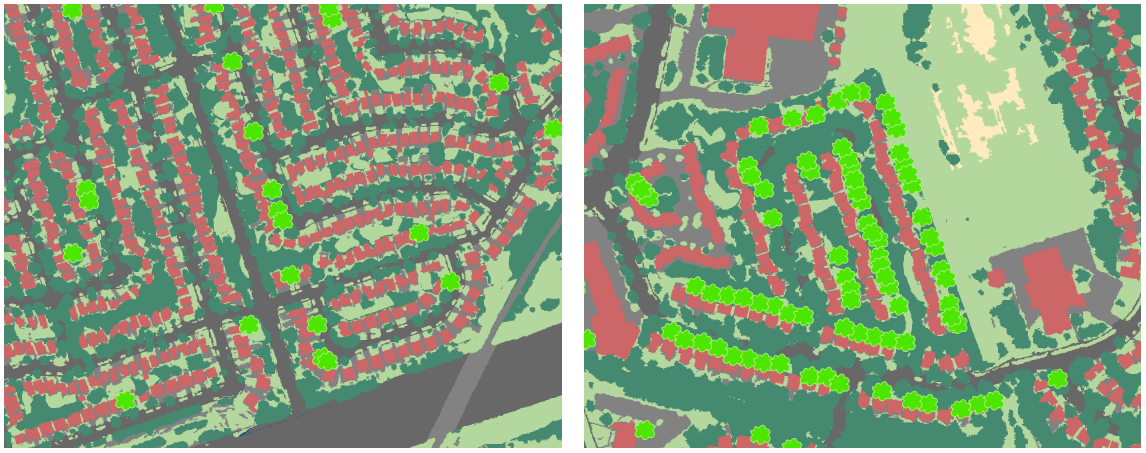

(a) Low density of ash trees. (b) High density of ash trees.

Notes: This Figure shows the land use classification in two neighborhoods of Scarborough (East of Toronto)—one with a relatively low density of ash trees (left panel); one with a relatively high density of ash trees (left panel). The data was produced in 2007 by Urban Forestry as part of an Urban Tree Canopy (UTC) Assessment. Land cover is characterized by the following classes: tree canopy (dark green), grass/shrub (lighter green), bare earth (sand), water (dark blue), buildings (red), roads (dark gray), other paved surfaces (light gray) and agriculture (yellow). The green symbols represent the location of public ash trees, as geolocated from their street addresses (Street Tree General Data, 2010).

Figure 2. Distribution of ash trees and transactions within the City of Toronto.

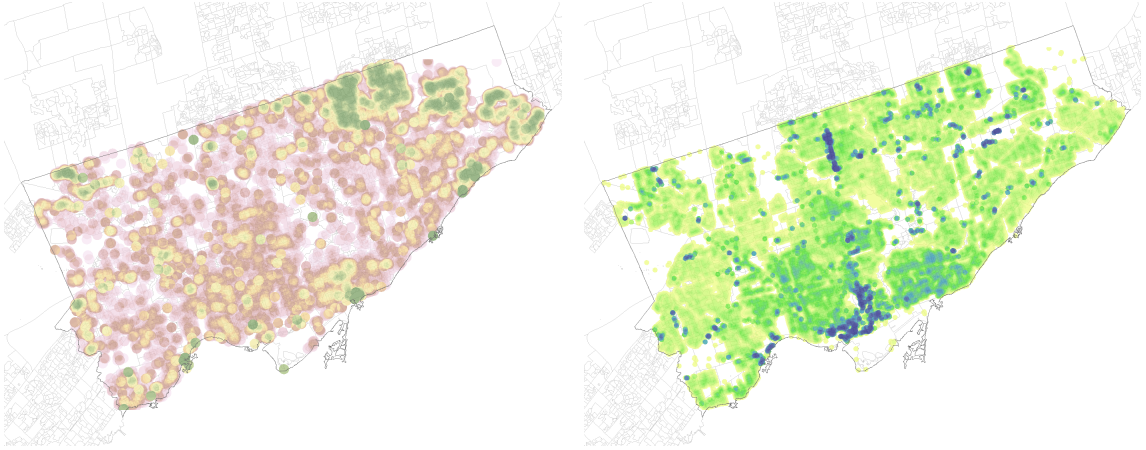

(a) Ash trees (density, 2010). (b) Transactions (density, 2007–2017).

Notes: The left panel shows the density of street ash trees managed by the city of Toronto (Street Tree General Data, Toronto, 2010); the right panel displays the density of property transactions between 2007 and 2017. Each color class represents a decile of density (from light pink to yellow to red on the left panel, from light yellow to green to blue on the right panel).

Figure 3. Ash trees and the evolution of the tree canopy—an illustration.

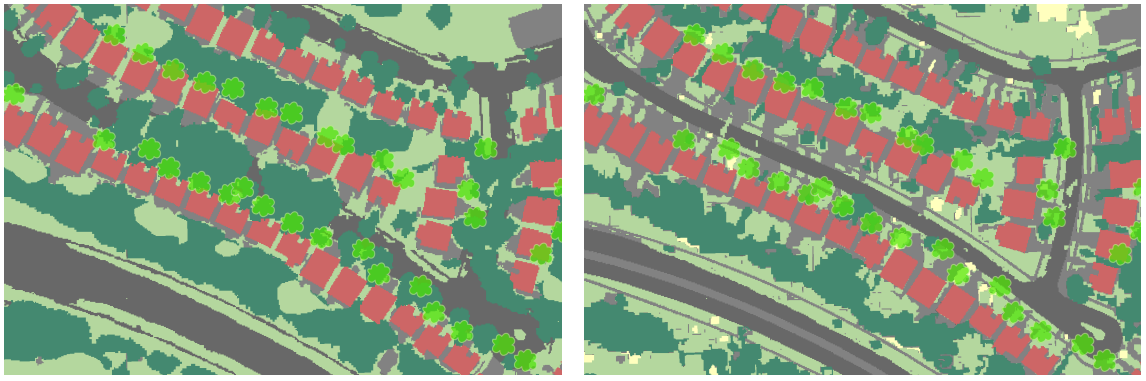

(a) 2007. (b) 2018.

Notes: This Figure shows the land use classification in a given neighborhood in the North-East of Toronto (Scarborough)—with a relatively high density of ash trees. The data was produced in 2007 (left panel) and 2018 (right panel) by Urban Forestry as part of an Urban Tree Canopy (UTC) Assessment. Land cover is characterized by the following classes: tree canopy (dark green), grass/shrub (lighter green), bare earth (sand), water (dark blue), buildings (red), roads (dark gray), other paved surfaces (light gray) and agriculture (yellow). The green symbols represent the location of public ash trees, as geolocated from their street addresses (Street Tree General Data, 2010).

Figure 4. The effect of ash tree density on the tree canopy between 2007 and 2018.

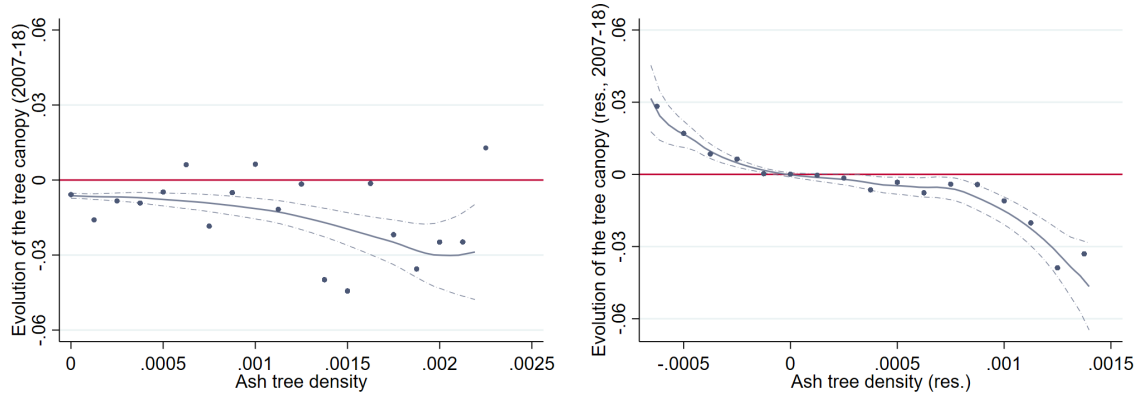

(a) Unconditional. (b) Conditional.

Notes: The left panel represents the relationship between the evolution of the area share of tree cover between 2007 and 2018 (as produced by Urban Forestry as part of an Urban Tree Canopy Assessment) and our ash tree density (number of street ash trees per area within a 10m buffer, as measured in 2010) across postcodes. We group transactions by bins of ash tree density: the dots represent the average evolution of the tree canopy within each bin. The right panel represents the same relationship in which the evolution of the area share of tree cover between 2007 and 2018 and the ash tree density are residualized: we regress both measures on a measure of street tree density, latitude, longitude, the land classification in 2007 (tree canopy, grass/shrub, bare earth, water, buildings, roads, other paved surfaces and agriculture) and ward fixed effects. The lines are locally weighted regression on all observations.

Figure 5. Correlation between transaction price and density of the tree canopy.

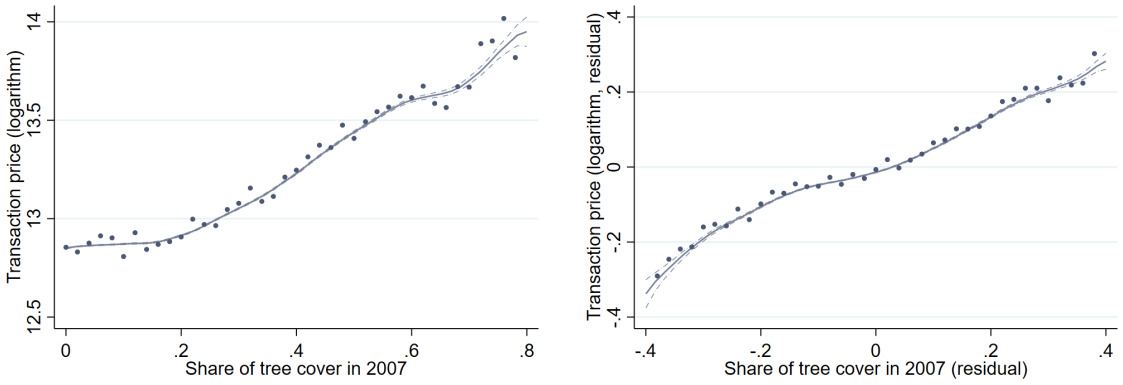

(a) Unconditional. (b) Conditional.

Notes: The left panel represents the relationship between the (logarithm) transaction price and our measure of tree cover at the postcode level (with a buffer of 10m around the postcode shape). We group transactions by bins of tree cover: the dots represent the average transaction price within each bin. The right panel represents the same relationship in which the (logarithm) transaction price and the tree cover within the postcode are residualized: we regress both measures on the number of bedrooms, the number of washrooms, the latitude, the longitude, ward fixed effects—all interacted with year fixed effects. The lines are locally weighted regression on all observations.

Figure 6. Correlation between Summer temperature and density of the tree canopy in 2018.

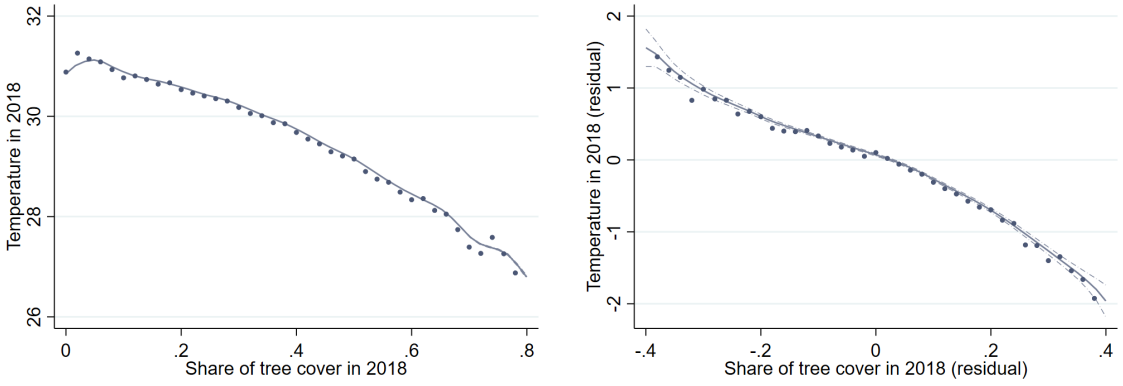

(a) Unconditional. (b) Conditional.

Notes: The left panel represents the relationship between the average temperature during the Summer in 2018 and our measure of tree cover at the postcode level (with a buffer of 10m around the postcode shape and in 2018). We group postcodes by bins of tree cover: the dots represent the average temperature within each bin. The right panel represents the same relationship in which the temperature and the tree cover within the postcode are residualized: we regress both measures on the latitude, the longitude, and ward fixed effects. The lines are locally weighted regression on all observations.

Figure 7. The cooling effect of urban forestry—an illustration.

(a) NDVI. (b) Temperature.

Notes: This Figure exploits Landsat 8 satellite imagery between June, 1st 2018 and September, 15th, 2018. The left panel shows the Normalized Difference Vegetation Index (NDVI) where green colors indicate a higher vegetation cover. The right panel shows the Land Surface Temperature (LST) where red colors indicate higher temperatures.

Table 1. Ash trees and the evolution of the tree canopy between 2007 and 2018.

	Tree cover (2007–2018)		
	(1)	(2)	(3)
Ash tree density	-12.23	-13.78	-13.96
	(1.349)	(1.365)	(1.372)
Street tree density		1.444	1.910
		(0.197)	(0.287)
Spruce tree density			1.189
			(1.305)
Elm tree density			3.408
			(2.042)
Maple tree density			-2.000
			(0.575)
Observations	45,520	45,520	45,520

Notes: Robust standard errors are reported between parentheses. The unit of observation is a postcode, and the dependent variable is change in tree cover between 2007 and 2018. All specifications include: ward fixed effects; latitude and longitude; and area shares from the land classification in 2007 (tree canopy, grass/shrub, bare earth, water, buildings, roads, other paved surfaces and agriculture).

Table 2. Descriptive statistics.

			Tree density	
	Mean	Stand. dev.	High	Low
Panel A: Transaction characteristics				
Transaction price	13.03	0.627	13.20	12.86
Number of bedrooms	1.981	1.351	2.331	1.630
Number of washrooms	2.182	1.114	2.479	1.886
Panel B: Land cover in 2007				
Tree canopy	0.220	0.191	0.380	0.060
Grass/shrub	0.152	0.121	0.181	0.123
Bare earth	0.009	0.083	0.001	0.017
Water	0.001	0.007	0.001	0.001
Buildings	0.225	0.161	0.192	0.259
Roads	0.161	0.165	0.114	0.207
Other paved surfaces	0.229	0.218	0.129	0.330
Agriculture	0.000	0.003	0.000	0.000
Panel C: Street trees				
Ash tree density (per sq. km)	78.28	263.2	89.59	66.98
Public tree density (per sq. km)	1,949	2,083	2,164	1,734
Observations		385,933	192,839	193,094

Notes: All statistics are computed using the baseline sample of transactions. The samples of high- and low-tree density are defined with respect to the median share of tree canopy as produced by Urban Forestry as part of an Urban Tree Canopy Assessment in 2007.

Table 3. The amenity value of trees—baseline specification.

	Transaction price (log)		
	(1)	(2)	(3)
Tree cover	-0.049	1.009	0.866
	(0.015)	(0.310)	(0.272)
Transaction controls	No	No	Yes
F-statistic	-	80.73	83.82
Observations	374,295	374,295	374,286

Notes: Standard errors are reported between parentheses and are clustered at the postcode × year level. Column 1 reports OLS results and columns 2-3 report the estimates from the IV specification in which tree cover is instrumented by the ash tree density. The unit of observation is a transaction, and the dependent variable is the (log) transaction price. All specifications are weighted by the inverse of the number of observations in a given postcode. The set of transaction controls include the number of washrooms and bedrooms interacted with year fixed effects. All specifications include: (i) postcode fixed effects; (ii) ward fixed effects interacted with year fixed effects; (iii) a measure of street tree density interacted with year fixed effects; (iv) latitude and longitude interacted with year fixed effects; (v) area shares from the land classification in 2007 (tree canopy, grass/shrub, bare earth, water, buildings, roads, other paved surfaces and agriculture) interacted with year fixed effects.

Table 4. The amenity value of trees—placebo specification (2002–2006).

	Transaction price (log)	
	(1)	(2)
Tree cover	-0.067	-0.197
	(0.020)	(0.388)
F-statistic	-	48.26
Observations	168,457	168,457

Notes: Standard errors are reported between parentheses and are clustered at the postcode × year level. Column 1 reports OLS results and column 2 reports the estimates from the IV specification in which tree cover is instrumented by the ash tree density. The unit of observation is a transaction, and the dependent variable is the (log) transaction price. All specifications are weighted by the inverse of the number of observations in a given postcode. All specifications include: (i) postcode fixed effects; (ii) ward fixed effects interacted with year fixed effects; (iii) a measure of street tree density interacted with year fixed effects; (iv) latitude and longitude interacted with year fixed effects; (v) area shares from the land classification in 2007 (tree canopy, grass/shrub, bare earth, water, buildings, roads, other paved surfaces and agriculture) interacted with year fixed effects.

Table 5. The amenity value of trees—robustness checks.

	Transaction price (log)		
	(1)	(2)	(3)
Panel A: No inference			
Tree cover	0.707	0.874	0.901
	(0.198)	(0.454)	(0.315)
F-statistic	115.44	79.72	51.66
Observations	311,261	240,448	168,598
Sample	7–11/14–17	7–10/15–17	7–9/16–17
Panel B: Long difference			
Tree cover	0.761	1.006	0.934
	(0.333)	(0.385)	(0.310)
F-statistic	64.93	55.48	41.26
Observations	21,264	18,404	14,312
Sample	7–11/14–17	7–10/15–17	7–9/16–17
Panel C: Sensitivity			
Tree cover	1.378	1.013	0.795
	(0.418)	(0.314)	(0.298)
F-statistic	30.33	65.12	48.07
Observations	370,556	374,286	374,286
Specification	Buffer: 20m	Winsorizing: 90%	Winsorizing: 99%
Panel D: Clustering			
Tree cover	0.866	0.866	0.866
	(0.345)	(0.290)	(0.485)
F-statistic	40.41	38.57	9.86
Observations	374,286	374,286	374,286
Clustering	Postcode	Ward × year	Ward

Notes: Standard errors are reported between parentheses and are clustered at the postcode × year level (except in Panel D). All columns report the estimates from the IV specification in which tree cover is instrumented by the ash tree density. In Panel A, C, D, the unit of observation is a transaction, the dependent variable is the (log) transaction price, and the specifications include: (i) postcode fixed-effects; (ii) ward fixed effects interacted with year fixed effects; (iii) a measure of street tree density interacted with year fixed effects; (iv) latitude and longitude interacted with year fixed effects; (v) area shares from the land classification in 2007 (tree canopy, grass/shrub, bare earth, water, buildings, roads, other paved surfaces and agriculture) interacted with year fixed effects; (vi) the number of washrooms and bedrooms interacted with year fixed effects. All specifications are weighted by the inverse of the number of observations in a given postcode. In Panel A, we restrict the sample to 2007–2011/2014–2017 in column 1, 2007–2010/2015–2017 in column 2, 2007–2009/2016–2017 in column 3. In Panel B, we apply the same sample restrictions and consider a specification in long difference in which all variables are collapsed at the postcode level. In Panel C, we explore variations around the baseline specification: a buffer of 20m around postcodes in column 1, a winsorizing at 90% for public and ash tree densities in column 2, a winsorizing at 99% for public and ash tree densities in column 3. In Panel D, we explore variations around the baseline clustering procedure: at the postcode level in column 1, at the ward × year level in column 2, at the ward level in column 3. There are about 50 wards in Toronto.

Table 6. The cooling effect of trees—temperature.

	Temperature (2018, log)		
	(1)	(2)	(3)
Tree cover	-0.359	-0.329	-0.270
	(0.059)	(0.053)	(0.043)
Controls	Ward	+ Extended	+ Temp. (2013, log)
F-statistic	101.1	100.2	95.90
Observations	45,501	45,501	45,501

Notes: Robust standard errors are reported between parentheses. The unit of observation is a postcode, and the dependent variable is the (log) temperature in 2018. Column 1-3 report the estimates from the IV specification in which the difference in tree cover between 2007–2018 is instrumented by the ash tree density at baseline. The specifications include: ward fixed effects (columns 1-3); latitude and longitude (columns 2-3); the density of publicly maintained trees (columns 2-3); area shares from the land classification in 2007 (columns 2-3); and the (log) temperature in 2018 (column 3).

Table 7. The cooling effect of trees—electricity consumption.

	Electricity differential (2014)		
	(1)	(2)	(3)
Tree cover	-23.71	-25.33	-14.59
	(7.123)	(7.701)	(5.481)
Controls	Ward	+ Extended	+ Electricity (2011)
F-statistic	37.64	39.25	40.28
Observations	19,948	19,948	19,909
	Electricity differential (2015)		
	(1)	(2)	(3)
Tree cover	-32.55	-32.79	-21.51
	(12.46)	(13.09)	(11.51)
Controls	Ward	+ Extended	+ Electricity (2011)
F-statistic	36.21	40.33	40.77
Observations	15,785	15,785	15,751

Notes: Robust standard errors are reported between parentheses. The unit of observation is a postcode, and the dependent variable is the electricity differential between Summer (June, July, August) versus the other months in 2014 (top panel) and in 2015 (bottom panel). Column 1-3 report the estimates from the IV specification in which the difference in tree cover between 2007–2018 is instrumented by the ash tree density at baseline. The specifications include: ward fixed effects (columns 1-3); latitude and longitude (columns 2-3); the density of publicly maintained trees (columns 2-3); area shares from the land classification in 2007 (columns 2-3); and electricity consumption in 2011 (column 3).

ONLINE APPENDIX

A Data appendix **32**

A.1 Satellite imagery 32

A.2 Tree canopy and land cover 34

A.3 Energy consumption 35

B Tree canopy and energy consumption **37**

B.1 Construction of the shade and shelter measures 37

B.2 Shade, shelter and energy consumption 39

A Data appendix

This section complements Section 1 with (i) a description of satellite imagery and vegetation/built-up indices; (ii) a characterization of the dynamics of urban forestry over time; and (iii) a description of the energy data.

A.1 Satellite imagery

Our baseline specification relies on land classifications provided by the Urban Forestry services of the City of Toronto based upon high-resolution satellite imagery and LiDAR information (City of Toronto, 2019). We however complement and validate these measures of land cover with satellite imagery (Sentinel 2, 2016–2020, 10m resolution; Landsat L8, 2013–2020, 30m resolution; Landsat L7, 2007–2012, 30m resolution).

Figure A1. Satellite imagery and vegetation/built-up indices (2018).

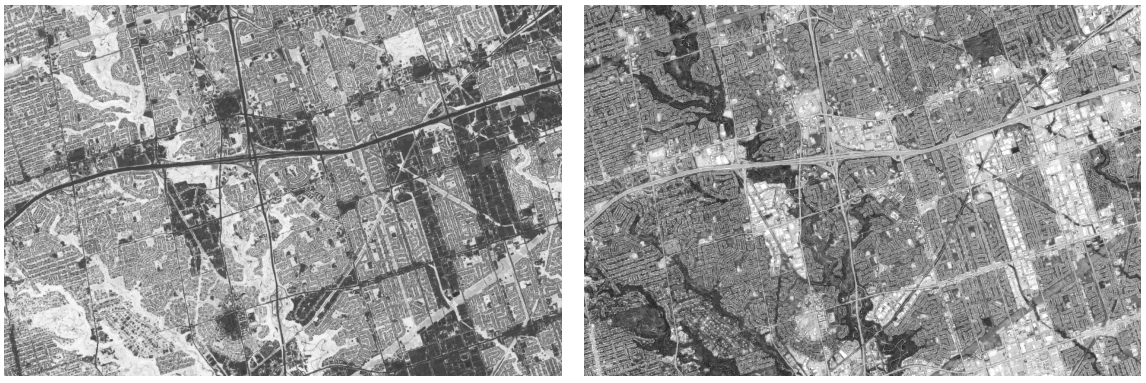

(a) NDVI. (b) NDBI.

Notes: This Figure displays vegetation/built-up indices constructed from a cloud-free mosaic of Sentinel imagery (S2, 10m resolution) covering May–September 2018 (North-East of Toronto). The Normalized Difference Vegetation Index (NDVI) is obtained by combining the reflection in the near-infrared spectrum (NIR) with the reflection in the red range of the spectrum (RED). The Normalized Difference Built-up Index (NDBI) is obtained by combining the reflection in the near-infrared spectrum (NIR) with the reflection in the short-wave infrared range of the spectrum (SWIR).

To construct vegetation, built-up and water indices, we proceed as follows for each collection of satellite imagery: (i) we isolate a summer period in any given year from June 1st to September 30th; (ii) we construct a cloud-free mosaic of images taken during this period; (iii) we construct a range of indices, most notably, Normalized Difference Vegetation Index (NDVI)—obtained by combining the reflection in the near-infrared spectrum (NIR) with the reflection in the red range of the spectrum (RED)— and the Normalized Difference Built-up Index (NDBI)—obtained by combining the reflection in the near-infrared spectrum (NIR) with the reflection in

the short-wave infrared range of the spectrum (SWIR); (iv) we consider the average indices within each postcode and every year covered by the collection. We illustrate the variation captured by NDVI and NDBI in Figure A1 (based on Sentinel S2 in 2018).

Figure A2. Validation of the measure of tree cover.

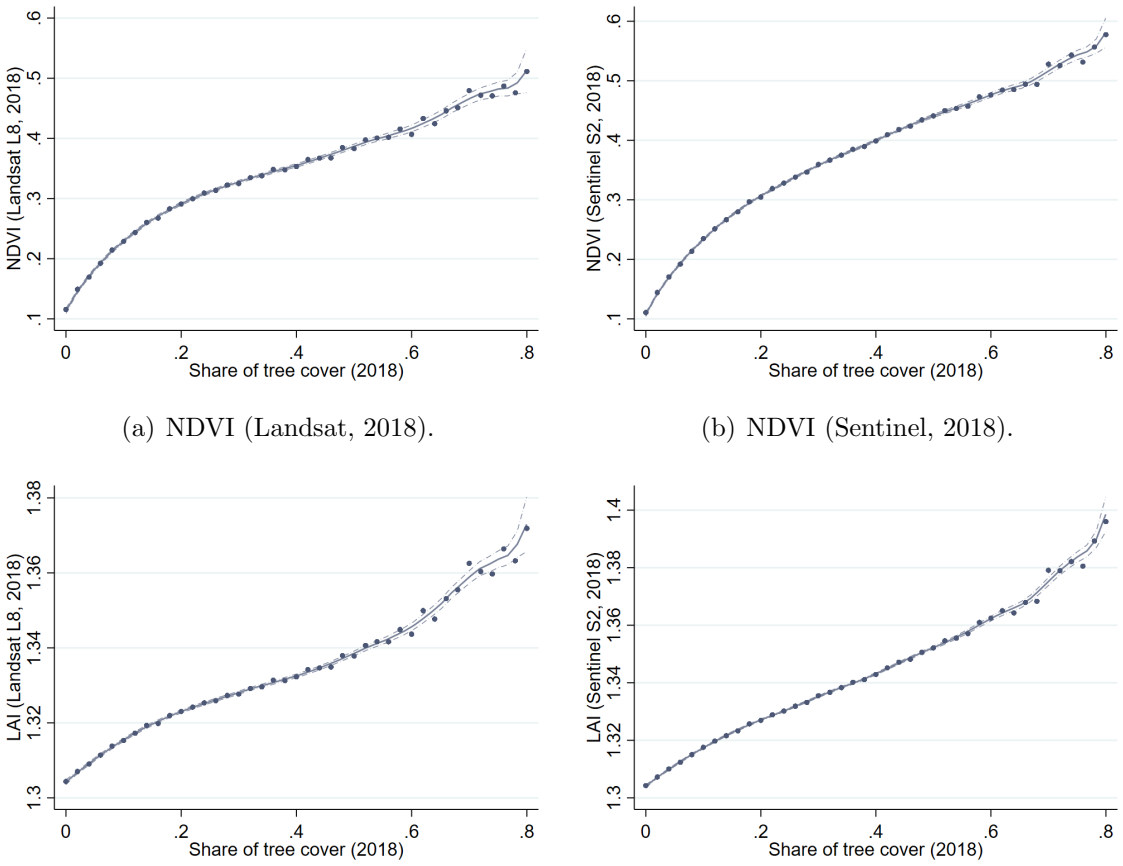

(a) NDVI (Landsat, 2018).

(b) NDVI (Sentinel, 2018).

(c) LAI (Landsat, 2018).

(d) LAI (Sentinel, 2018).

Notes: This Figure correlates the measure of tree cover produced by Urban Forestry as part of an Urban Tree Canopy (UTC) Assessment in 2018 with standard vegetation indices extracted from recent satellite imagery. Panels (a) and (b) correlate the area share of tree canopy in 2018 with the Normalized Difference Vegetation Index (NDVI) across postcodes. The NDVI is obtained by combining the reflection in the near-infrared spectrum (NIR) with the reflection in the red range of the spectrum (RED). Panels (c) and (d) correlate the share of tree coverage in 2018 with the Leaf Area Index (LAI) across postcodes. Panels (a) and (c) rely on a cloud-free mosaic of Landsat imagery (L8, 30m resolution) covering May–September 2018. Panels (b) and (d) rely on a cloud-free mosaic of Sentinel imagery (S2, 10m resolution) covering May–September 2018.

We use these indices to validate the land classification data and shed some light on the dynamics of urban forestry over our period of interest. In Figure A2, we correlate the measure of tree cover produced by Urban Forestry as part of an Urban Tree Canopy (UTC) Assessment in 2018 with our vegetation indices, as extracted from recent satellite imagery (Landsat L8 and Sentinel S2). We see that there is

a very strong, positive, quasi-linear relationship between the area share covered by the tree canopy and the vegetation indices based on average reflectance across the visible, infra-red, near infra-red spectrum.

A.2 Tree canopy and land cover

In this section, we leverage the previous vegetation indices to gain some insight into the dynamics of urban forestry between 2007 and 2020. More specifically, we run an event-study specification for the relationship between vegetation indices, I_{pt} in postcode p at time t and our measure of exposure to the EAB infestation:

$$I_{pt} = \sum_{\tau=2009}^{\tau=2020} \beta_\tau A_{p,2010} \times \mathbb{1}_\tau + \mathbb{X}_{pt} + \eta_p + \varepsilon_{pt},$$

where $\mathbb{X}_{pt}$ includes: a measure of street tree density; ward fixed effects; latitude, longitude; dummies for the land classification in 2007 (tree canopy, grass/shrub, bare earth, water, buildings, roads, other paved surfaces and agriculture)—all interacted with year fixed effects. We report the outcome of this specification in Figure A3.

Figure A3. The effect of ash tree density on the tree canopy over time.

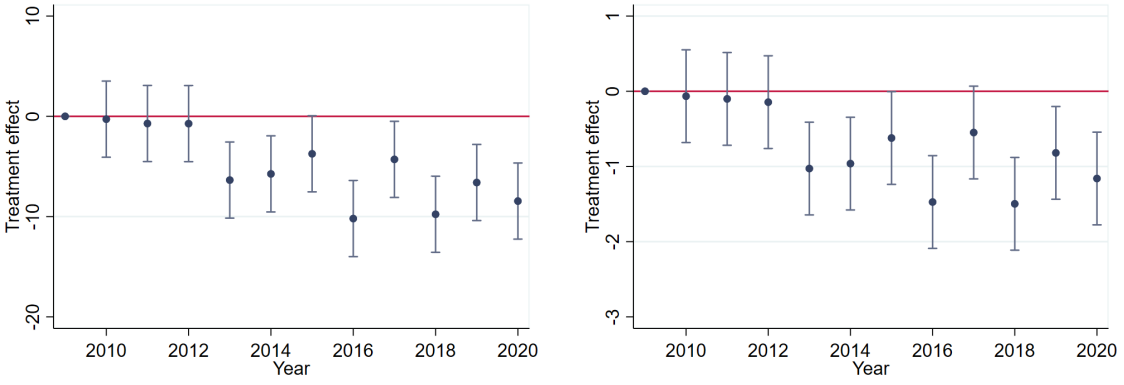

(a) NDVI. (b) LAI.

Notes: This Figure shows the estimated treatment effect of ash tree density on the tree canopy over time. More specifically, we regress the Normalized Difference Vegetation Index (NDVI, left panel) and the Leaf Area Index (LAI, right panel) across postcodes on: a measure of ash tree density (number of street ash trees per area within a 10m buffer, as measured in 2010); a measure of street tree density; ward fixed effects; latitude, longitude; dummies for the land classification in 2007 (tree canopy, grass/shrub, bare earth, water, buildings, roads, other paved surfaces and agriculture)—all interacted with year fixed effects. The reported coefficients are the ones in front of the measure of ash tree density interacted with years, and vertical lines show 95 percent confidence intervals. The NDVI is obtained by combining the reflection in the near-infrared spectrum (NIR) with the reflection in the red range of the spectrum (RED) and relies on a cloud-free mosaic of Landsat imagery (L8, 30m resolution) covering May–September from 2009 to 2020. The LAI uses the same satellite imagery and is obtained by combining the same bands.

One can see that the differential dynamics of vegetation indices across neighborhoods is noisy, but the treatment effect seems most pronounced from 2012 onward.

A.3 Energy consumption

Energy consumption is reported in kilowatt hours (kWh) adjusted for line losses over the billing period. The days of service in a billing period range between 1 and 2 months (see Figure A4) and we know the start and end date of each billing period which varies across households. To calculate the average monthly energy consumption in postcode p, month m and year t, we construct a daily panel of each household i's average daily energy consumption and estimate:

$$e_{ipmt} = \alpha_i + E_{pmt} + \epsilon_{ipmt}$$

where the fixed effects E_{pmt} capture the average daily energy consumption in postcode p for a given month m of year t. To derive a measure e_{pmt} of the average energy consumption per month and year, we multiply the average daily energy consumption e_{ipmt} by the number of days in the respective month m. One nice feature of our electricity data is that we can condition the estimation on energy meter fixed effects, α_i, which absorb all time-invariant house and occupant characteristics. The latter control, for example, for the energy efficiency of the house.

Figure A4. Distribution of the days of service intervals across billing periods.

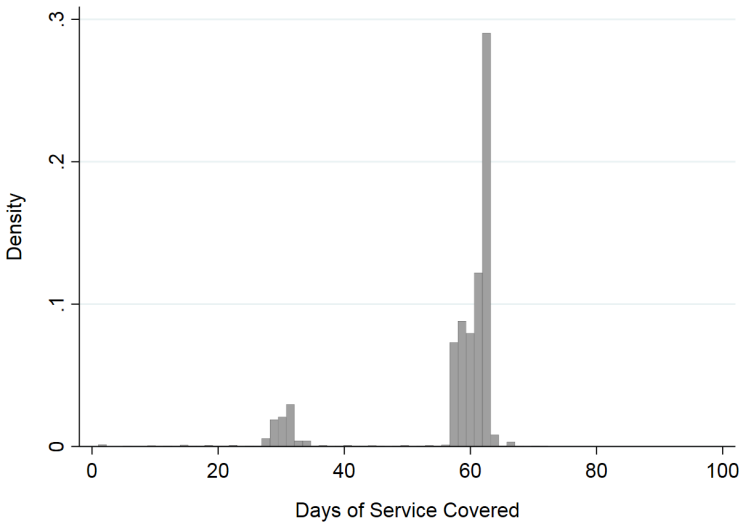

Notes: This Figure represents the distribution of the days of service intervals across billing periods and is based on residential energy meters between 2012 and 2015.

There are important seasonal patterns in energy consumption which we illustrate in Figure A5. Electricity consumption is high in the summer months, due to the use of air conditioning. Between November–April, electricity consumption is a mix

of light and electrical heating, even though natural gas is the most common source of heating fuel. Consequently, we would expect trees to have more pronounced electricity consumption effects in the summer. Natural gas is used for heating during these winter months and there is indeed a significantly higher usage of natural gas in these months with a spike in January and February, the coldest months.

Figure A5. Electricity and gas consumption over time.

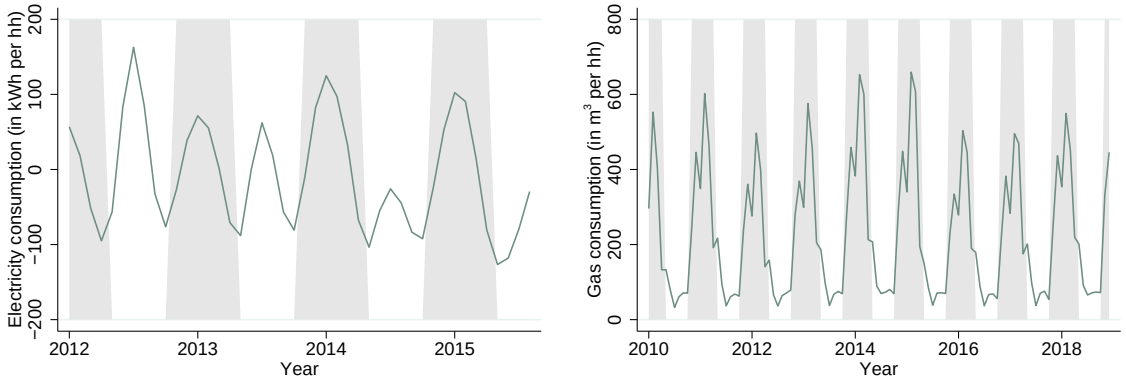

(a) Electricity.

(b) Natural gas.

Notes: The left panel of the graph shows the regression adjusted average monthly electricity consumption measured in kWh across postcodes in Toronto. The right panel shows the average monthly consumption of natural gas measured in cubic meters across postcodes in Toronto. Gray shaded areas indicate winter months, i.e., November–April.

B Tree canopy and energy consumption

This section provides complements to Section 4. More specifically, we analyze energy consumption during episodes of high temperatures (resp. wind chill) as a function of the solar-shading potential (resp. wind-sheltering potential) of the local urban forestry.

B.1 Construction of the shade and shelter measures

We first focus on the construction of two measures, the *solar-shading potential* and the *wind-sheltering potential*.

Figure B1. Shading effect of trees—creation of the time-dependent variable.

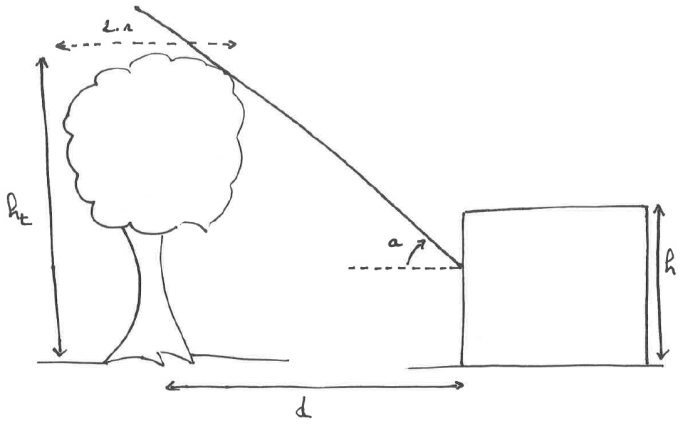

Notes: This Figure schematically represents the parameters used in order to derive the measure $Shade_{imh}$ which depends on a month of the year m, a time of the day h, and the surroundings of property i. We calculate the shade, $Shade_{imh}$, as the percentage of the house front covered in shade by the nearest tree (distance d) in the direction as implied by the time of the day h, and with the sun angle a as implied by the time of the day h and month m. We consider a house front to be between 2 and 7 meters, we assume that trees are $h_t = 20$ meters high with a crown radius of $r = 5$ meters.

For the shading potential of the neighboring tree canopy, we compute the measure S_{im} for property i and month m of a given year as,

$$S_{im} = \frac{\int sun_{mh} \times Shade_{imh} dh}{\int sun_{mh} dh}.$$

h is a time of the day, sun_{mh} is the potential sun exposure at time h in month m and $Shade_{imh}$ is a measure of shade induced by the presence of trees around property i at time h in month m. The variable $Shade_{imh}$ is constructed by reconstituting the month-specific solar angle $a_m(h)$ and sun direction $d_m(h)$ as a function of time h. At time h, we select all trees in direction $d_m(h)$ originating from the centroid of a property. We then calculate the share of the property which is in the shade

of these trees, $Shade_{imh}$, exploiting the distance to the trees and the solar angle. This computation requires several assumptions regarding the height of a tree, the diameter of its crown, and the height and width of a property. We provide additional details about the computation in Figure B1.

Figure B2. Sheltering effect of trees—creation of the time-dependent variable.

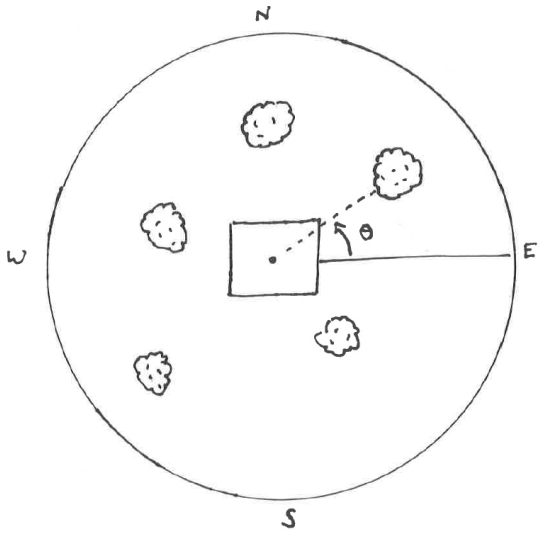

Notes: This Figure schematically represents the parameters used in order to derive the measure $Tree_{\theta i}$ used to construct the sheltering effect of trees. We combine the surroundings of property i with the direction of wind θ as follows: $Tree_{\theta i}$ is a dummy equal to 1 if there is a tree in direction θ and within 20 meters of the property.

To capture the sheltering potential of trees in vicinity to property i in month m of a given year, we compute

$$W_{im} = \sum_{\theta} w_{\theta m}(1 - Tree_{\theta i})p_{\theta t}.$$

$w_{\theta m}$ is the wind chill equivalent temperature (WCET) used by Environment Canada, given the temperature in month m and the average wind speed from direction θ; $Tree_{\theta i}$ is a dummy equal to 1 if there is a tree in direction θ and within 20 meters of the property; $p_{\theta t}$ is the probability that the wind originated from direction θ in month m. We also compute a counterfactual measure for the wind chill equivalent temperature (WCET), ignoring the neighboring tree:

$$W^c_{im} = \sum_{\theta} w_{\theta m}p_{\theta m}$$

We leave additional details of the computation to Figure B2.

B.2 Shade, shelter and energy consumption

Empirical strategy To estimate the (local) cooling effect of urban forestry, we rely on a different empirical strategy exploiting short-run fluctuations in weather conditions. We run a simple difference-in-differences specification at the postcode level for all months m in year t between January 2011 and December 2015. Letting p denote a postcode, m a month and t a particular year, we estimate the following equation:

$$\ln(E_{pmt}) = \alpha + \beta_2 S_{pm} \times Temp_t + \beta_1 S_{pm} + \beta_0 Temp_t + \delta_p + \nu_m + \mu_t + \varepsilon_{pmt} \quad (4)$$

where $\ln(E_{pmt})$ is the (log) measure of energy consumption in a postcode/date. The measure S_{pm} captures the shade implied by surrounding trees in month m, thus depending on seasonal solar angles. The measure $Temp_t$ is a dummy equal to 1 during episodes of exceptionally high temperatures (within the top decile recorded between May and September). The identification of parameters β hinges on excess energy savings during extreme weather episodes in properties with higher *solar-shading potential*. ν_m and μ_t are year and month fixed effects that may also be interacted.

We run a similar regression during low-temperature episodes in order to estimate the wind-sheltering effect of urban forestry.[15] Letting p denote a postcode, m the month, and t the year, we estimate the following equation:

$$\ln(E_{pmt}) = a + bW_{pmt} + cW^c_{pmt} + \delta_p + \nu_m + \mu_t + \varepsilon_{pmt} \quad (5)$$

where the measures W_{pt} and W^c_{pt} are measures of wind chill, W_{pt} accounting for the presence of surrounding trees and prevailing wind directions during month t. The identification of parameter b hinges on excess energy savings during extreme weather episodes in properties with higher *wind-sheltering potential*. As before, ν_m and μ_t are year and month fixed effects that may also be interacted.

Results We now quantify the energy-saving effect of trees. For illustrative purposes, we will use graphs to show our main findings and we leave the underlying regression models in Tables B1 and B2. Panel (a) of Figure A5 describes the relationship between excess energy consumption during heat waves and the relative positioning of trees. We estimate the conditional correlation between excess energy

[15] Since 70 percent of energy used in the residential sector comes from oil or gas (Mohareb and Mohareb, 2014), we expect a stronger effect of wind-sheltering on gas consumption. However, some heating is electric and we still expect to find some effect.

consumption and surrounding trees as follows. We regress the postcode energy consumption on a dummy for heat waves, the number of trees in a certain direction (East, North, West, South) and their interaction, while controlling for time-fixed effects and postcode fixed-effects. Figure A5 reports the energy premium guaranteed by the presence of trees during heat waves (the interaction term) in all four directions. The energy premium associated with the presence of a tree is not negligible in all directions, but even more so in the East and South where shade is likely to provide cooling.

Figure B3. Excess energy consumption in extreme weather episodes and the relative positioning of trees.

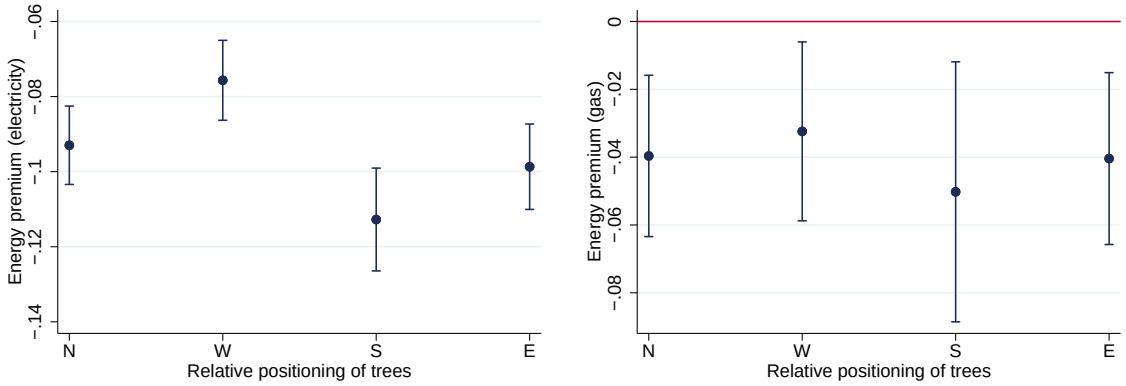

(a) Heat waves.

(b) Wind chill.

Notes: This Figure represents the conditional correlations between energy consumption and the number of trees in each of the four main directions from the property. See Section 2 for additional details.

Panel (b) of Figure A5 replicates the previous exercise for episodes of extreme cold. We regress the postcode energy consumption on a dummy equal to 1 if the wind chill equivalent temperature is lower than 0 Celsius degrees, the number of trees in a certain direction (East, North, West, South) and their interaction, while controlling for time-fixed effects and postcode fixed-effects. As expected, the energy premium associated with the presence of a tree is smaller than it is for extreme heat episodes. This is because fossil fuels are the dominant energy source while electricity is less common. That said, the estimated effect is significantly different from 0 except when the tree is in the direction to the East. One explanation could be that prevailing winds in Toronto blow from the West, South or North, but rarely from the East.

Table B1. Energy consumption and the cooling effect of trees.

Energy consumption	(1)	(2)	(3)
Heat wave	.1073	.0437	.0437
	(.0137)	(.0109)	(.0109)
Heat wave × Shade	-.2997	-.3154	-.3157
	(.0518)	(.0528)	(.0528)
Observations	2,271,628	2,271,628	2,271,628
Fixed effects (postcode)	No	Yes	Yes
Fixed effects (time)	Year	Month/year	Month/year
Controls (historical temperature)	No	No	Yes

Standard errors are reported between parentheses and are clustered at the date-level. The unit of observation is a date × postcode.

Table B2. Energy consumption and the sheltering effect of trees.

Energy consumption	(1)	(2)	(3)
Wind chill (no shelter)	-.0047	-.0039	-.0038
	(.0004)	(.0005)	(.0005)
Wind chill (shelter)	.0015	.0016	.0016
	(.0003)	(.0003)	(.0003)
Observations	2,161,759	2,161,759	2,161,759
Fixed effects (postcode)	No	Yes	Yes
Fixed effects (time)	Year	Month/year	Month/year
Controls (historical temperature)	No	No	Yes

Standard errors are reported between parentheses and are clustered at the date-level. The unit of observation is a date × postcode. *Wind chill* is a measure of felt temperature accounting for wind speed (and shelter in the second row).